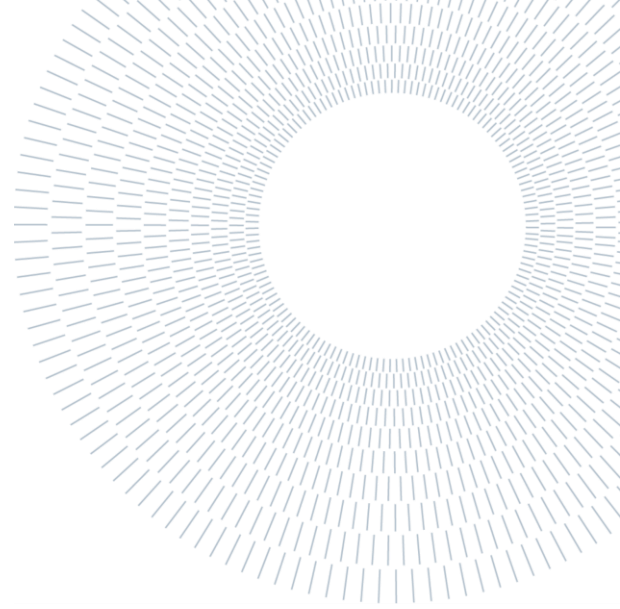




POLITECNICO
MILANO 1863

SCUOLA DI INGEGNERIA INDUSTRIALE
E DELL'INFORMAZIONE



EXECUTIVE SUMMARY OF THE THESIS

The integration of wind and solar renewable energy sources into 3 kV DC railway systems.

TESI MAGISTRALE IN ELECTRICAL ENGINEERING – INGEGNERIA ELETTRICA

AUTHOR: MARCO ALESSANDRO CERVI

ADVISOR: MORRIS BRENNNA

ACADEMIC YEAR: 2021-2022

1. Introduction

The focus of this work is to investigate the effects of integrating the traction power substations (TPSSs) of the 3 kV DC railway system with wind and solar renewable generators, under different conditions of railway traffic and train mission profiles, and for different availabilities of wind resource and solar irradiance. This work is also intended to provide an overview of the main elements of PV systems, wind generators, the 3 kV DC railway systems, and the DC railway microgrid concept that involves the “smartization” of current railway infrastructure to accommodate distributed renewable generators, charging stations for electric vehicles (EVs), and energy storage and energy management systems. Finally, simulations conducted in MATLAB® and Simulink-SIMSCAPE™ are presented.

2. The 3 kV DC railway system: current structure and future developments

Conventional 3 kV DC railway systems, covering almost 12000 km of the Italian railway (followed by the 25 kV 50 Hz that accounts for 1300 km), are characterized by a relatively simple and advantageous structure consisting of diode-based traction power substations that draw the power from the main grid at 132 kV and convert it to 3 kV DC to power sections of overhead catenary (or contact line) that feed the traction loads, as depicted in Figure 1. In such DC systems, the contact line can be powered in parallel by the TPSSs without interrupting the mechanical and electrical continuity of the traction circuit, whereas in AC railway systems, section breaks are required for phase rotation needed for balancing the power drawn from the main grid, causing train deceleration and increased wear of the pantograph.

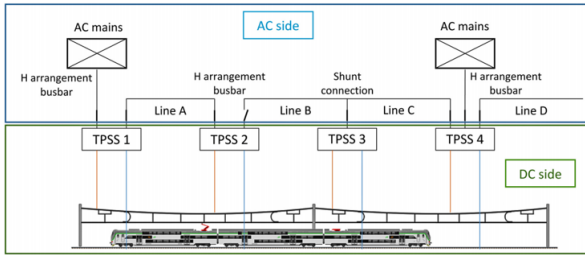


Figure 1: Basic structure of the 3 kV DC railway [1].

Due to their intrinsic functionalities, 3 kV DC railway systems are deemed by experts to be immediately eligible for the integration of other DC elements such as distributed wind and solar renewable energy sources (RES) that possess a DC section for direct connection, EV charging infrastructure, and energy storage systems, giving rise to the DC railway microgrid concept.

In this regard, the following work considers the connection of a 1.5 MW photovoltaic system and a 1.5 MW wind farm to two consecutive TPSSs that supply a 3 kV DC double track circuit.

3. The ETR1000 high-speed train

The traction vehicle considered for the simulations is the Italian high-speed train ETR1000, which serves as a good example of a high-power traction load, reaching a top speed of 300 km/h under 3 kV DC power supply and developing a maximum power at the wheels of 6.9 MW.

3.2 Mechanical model

With the objective to simulate the electrical power exchange within the 3 kV DC railway network supplying the traction loads in various modes of operation, the train is initially modeled using theoretical formulas and empirical results in the domain of railway traction mechanics, as well as manufacturer data of the traction vehicle and of the track, to represent the longitudinal dynamics of the vehicle (speed, position, and acceleration profiles) and the mechanical power at play. The electrical model is then implemented, building on the results provided by the mechanical model, to obtain the electrical power and current absorbed by the train (or injected, when regenerative braking is implemented) and the voltage profile at the pantograph, as well as the relevant electrical parameters of the traction circuit. The mechanical

and electrical characteristics of the train and of the track are determined using the data in Table 1 [1,2].

| | |
|-------------------------------------|-----------|
| Static mass | 501000 kg |
| Equivalent mass | 521040 kg |
| Max. acceleration | 0.7 m/s |
| Max. deceleration | 1 m/s |
| Adhesion coefficient | 0.33 |
| Max. traction power at the wheels | 6.9 MW |
| Max. braking power at the wheels | 5.6 MW |
| Number of total/motorized wheelsets | 32/16 |
| Maximum speed | 300 km/h |
| Track gradient | +/- 5.7 ‰ |

Table 1: main mechanical parameters of the ETR1000 and of the track.

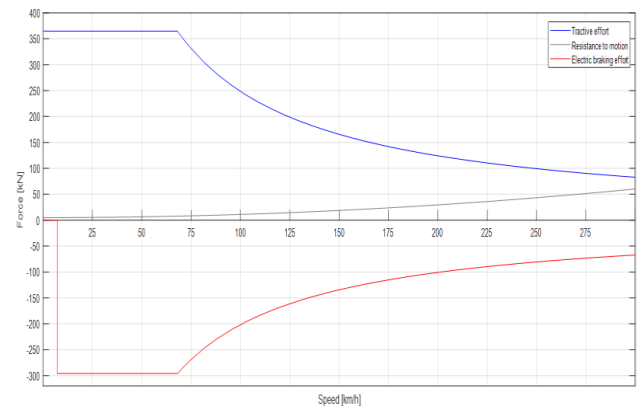


Figure 2: Tractive and braking characteristics of the ETR1000.

3.3 Electrical model of the traction load and of the track

The values of electrical power and current absorbed by the trains (or injected, when regenerative braking is implemented) and the voltage profile at the pantograph, as well as the resistances associated with the rails and the contact line for different train mission profiles are determined and fed as inputs to the simulation model starting from the data presented in Table 2 and considering the bilateral power supply of a double track as shown in Figure 3.2.

| | |
|------------------------------------------|--------------|
| Overall efficiency of the traction chain | 0.842 |
| Overall efficiency of the braking chain | 0.8 |
| Power absorbed by auxiliary services | 220 kW |
| Rails kilometric resistance | 0.00625 Ω/km |
| Contact line kilometric resistance | 0.0295 Ω/km |
| Length of the track | 20 km |
| TPSS voltage | 3.6-3.7 kV |
| Minimum line voltage | 2000 V |

Table 2: main electrical parameters of the traction load and traction circuit.

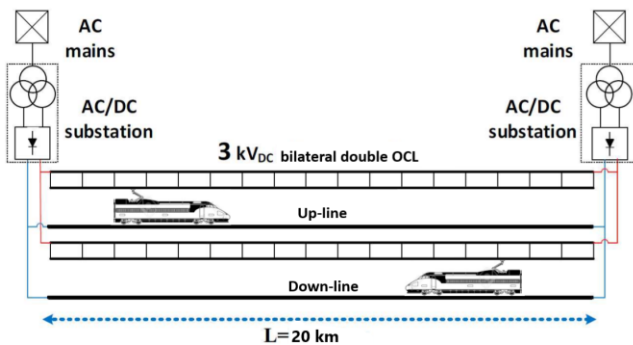


Figure 3: Double track with bilateral power supply.

As an example, the main results produced from the mechanical and electrical model relative to the ETR1000 on start-up on the up-line are illustrated in the following figures.

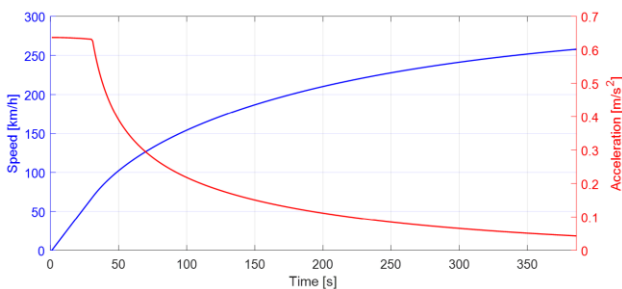


Figure 4: Up-line speed and acceleration profile

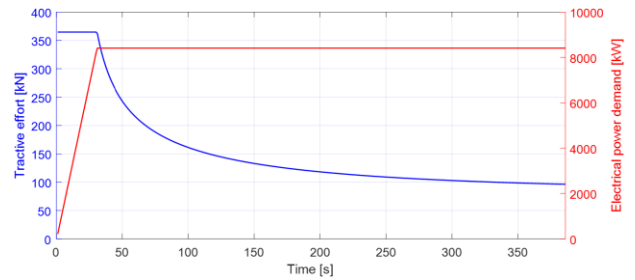


Figure 5: ETR1000 tractive effort and electrical power demand.

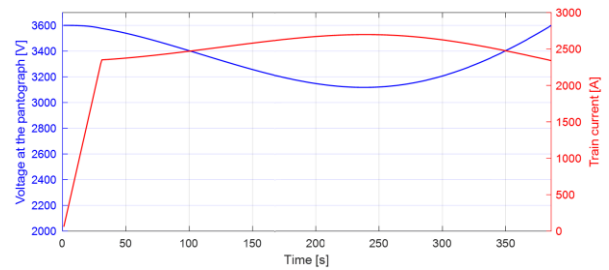


Figure 6: ETR1000 start-up on up-line: voltage and current profile

As a means of comparison, the traction circuit resistances for different train mission profiles are reported in Figure 6.

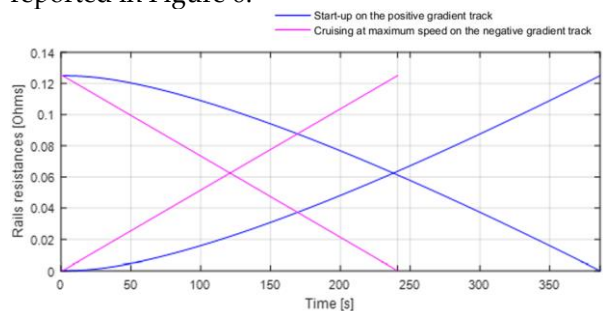


Figure 7: Rails and contact line bilateral resistances.

The following paragraphs summarize the choice of the PV and wind generators to be connected to the TPSSs to aid in the power supply of the traction loads.

4. The PV system

The considered photovoltaic generator is characterized by a rated power of 1.5 MWp under standard test conditions and produces a rated DC voltage of 711 V, which is in line with the typical PV-side voltages of utility-scale PV systems [3]. To obtain the desired specifications, it is comprised of 371 strings of 13 series-connected PV modules. PV module data is summarized in Table 3.

| | |
|-----------------------|--------------------------|
| Module type | SunPower SPR-315NE-WHT-D |
| Peak power | 305.07 Wp |
| MPP voltage | 54.7 V |
| MPP current | 5.76 A |
| Open-circuit voltage | 64.6 V |
| Short-circuit current | 6.14 A |

Table 3: PV module data.

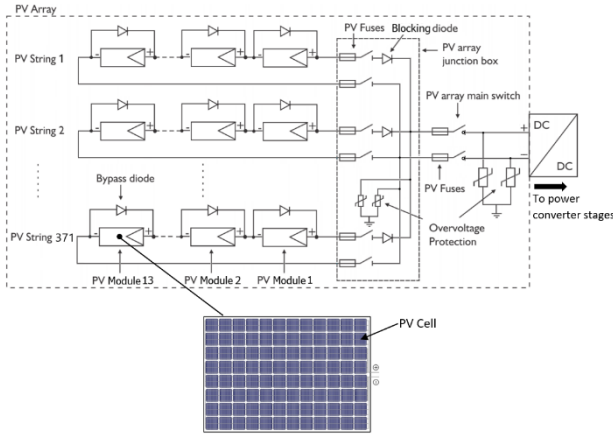


Figure 8: : PV field diagram.

To deliver the maximum power from the available solar irradiance and to boost the output voltage from 711 V to the TPSS voltage of 3.6 kV, a boost converter cascaded by an isolated boost full bridge (IBFB) converter are used. The first converter performs maximum power point tracking by implementing a Perturb & Observe algorithm, while the IBFB converter stabilizes the boost converter output voltage to 1 kV and provides the required voltage step-up function by means of a high-frequency transformer as illustrated in Figure 10.

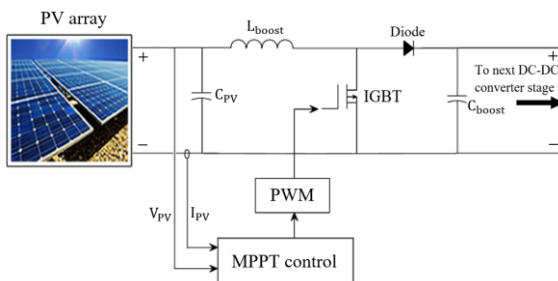


Figure 9: Boost converter topology.

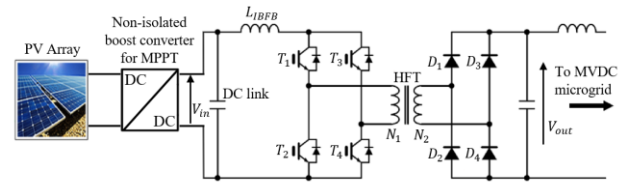


Figure 10: Isolated boost full-bridge converter.

Based on common and reasonable values of current and voltage ripple, the main electrical parameters of the converters are the following:

- Boost converter input inductance: 5 mH
- Boost converter output capacitance: 5 mF
- Boost converter switching frequency: 10 kHz
- IBFB converter output inductance: 5 mH
- IBFB converter output capacitance: 10 mF
- IBFB converter switching frequency: 10 kHz

5. The wind farm

The renewable generating unit considered for the connection to the TPSS is a 1.5 MW wind farm comprised of 3 individual wind turbines of rated power of 500 kW. Each turbine is sized by using theoretical equations in the domain of wind turbine aerodynamics as well as empirical formulas typical data made available by manufacturers. The generator choice is the permanent magnet synchronous generator (PMSG), widely used in wind power generation applications due to its capabilities for variable speed operation and the consequent advantages in wind turbine control [4]. The main parameters of the wind turbines, designed to operate in wind conditions typical of central Italy, are reported in Table 4.

| | |
|----------------------|-------------------------------------|
| Rated power output | 500 kW |
| Rated wind speed | 10 m/s |
| Cut-in wind speed | 2.5 m/s |
| Cut-out wind speed | 20 m/s |
| Hub height | 45 m |
| Rotor radius | 25.4 m |
| Blade pitch | 0° fixed |
| Rotational speed | Variable below the rated wind speed |
| Electrical generator | PMSG |
| Overall efficiency | 0.84 |

Table 4: Wind turbine data.

In the simulation, the wind generator is modeled by means of a simplified mathematical function based on the theoretical equations of wind turbine operation, that implements the maximum power coefficient between the cut-in and rated wind speed, and saturates the power output to the rated value above the rated wind speed. When the wind speed exceed the cut-in value, the power output is set to zero.

6. Simulation of the 3 kV DC railway system with and without RES

The model of the 3 kV DC railway system, complete with the traction loads and PV and wind generators, is illustrated in Figure 11. The main subsystems of the model are shown in Figures 12-15.

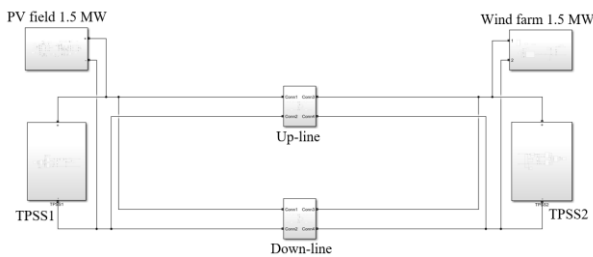


Figure 11: 3 kV DC double track with two TPSSs and renewable generators.

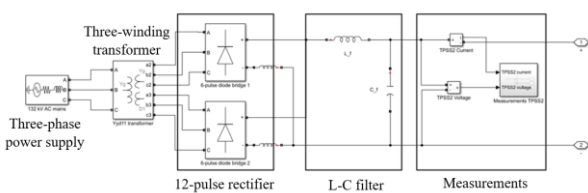


Figure 12: TPSS subsystem.

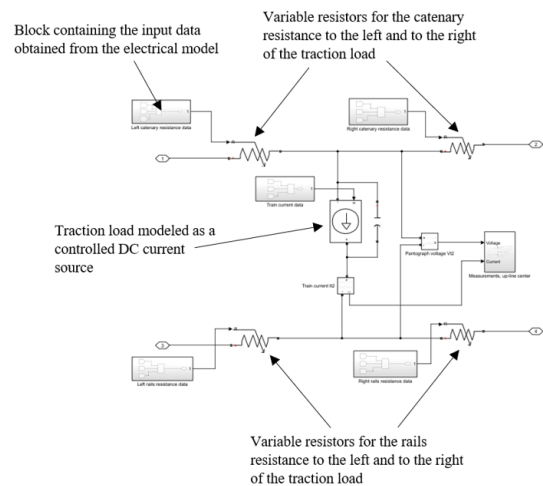


Figure 13: Traction line and load subsystem.

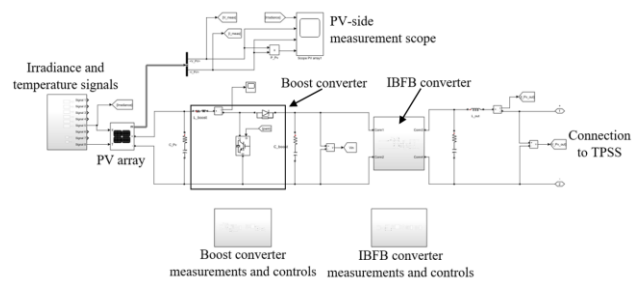


Figure 14: PV system block.

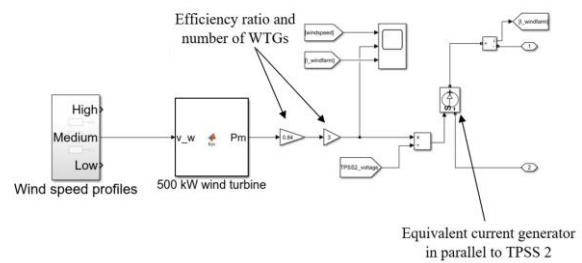


Figure 15: Wind farm subsystem.

The following paragraphs illustrate the main simulation results for two different scenarios of railway traffic with and without RES availability. The first scenario involves two trains traveling at maximum speed, one on each track (up-line and down-line) in opposite directions and with zero temporal offset between departures, the second scenario is related to one train traveling at maximum speed on the down-line. To allow the simulations to run in reasonable amounts of time, the model input signals have been compressed (by a factor of 400), hence the simulation time axes in the following plots.

6.1 Two trains traveling at maximum speed, one on each track

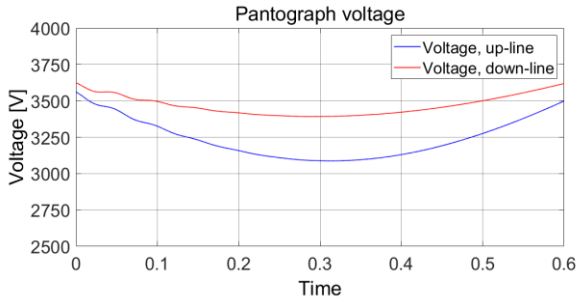


Figure 16: line voltages.

The line voltages (i.e., the catenary voltage at the pantograph) take on a parabolic trend that is typical of the bilateral power supply. As shown in Figure 16, the voltage drop in the up-line is greater than that of the down-line due to the higher current and power demand associated with the uphill gradient. The minimum voltages occur at the midpoint of the line, reaching 3070 V for the up-line and 3400 V for the down-line, both within the minimum voltage limits as prescribed by regulations (EN 50163).

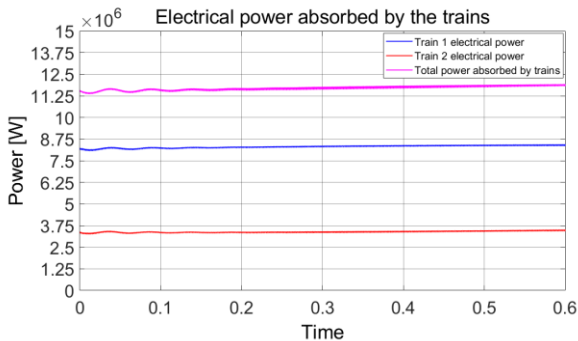


Figure 17: power absorption.

The considerable power demand given by the simultaneous presence of the trains traveling at maximum speed in the railway line can be seen in Figure 17. The total power absorbed by the traction loads is approximately 11.32 MW, with the train on the up-line absorbing 8.45 MW (with a peak current absorption of 2700 A) and the train on the down-line absorbing less than half, approximately 3.5 MW (with peak current absorption of 997 A).

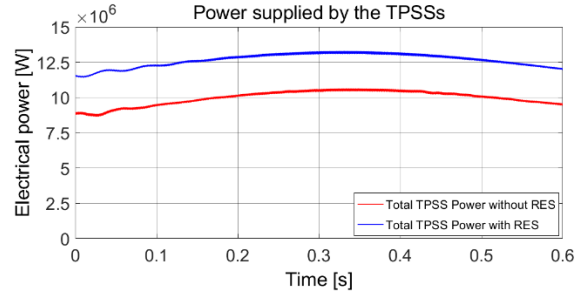


Figure 18: Total TPSS power with and without RES.

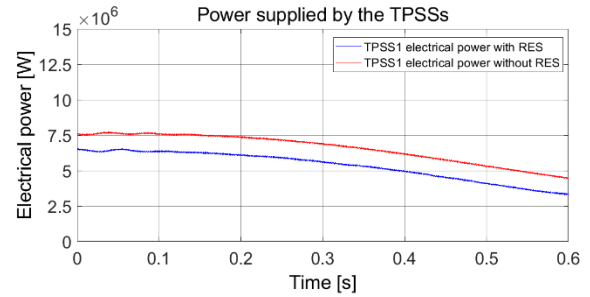


Figure 19: TPSS 1 power with and without RES.

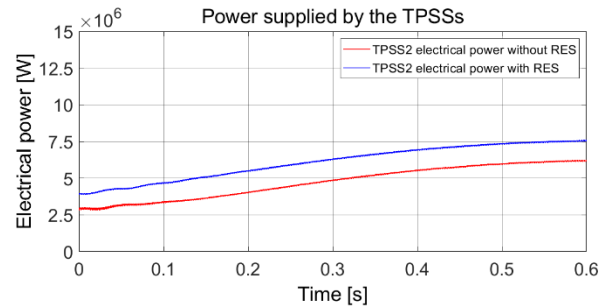


Figure 20: TPSS 2 power with and without RES.

The contribution of the renewable generators can be appreciated from Figure 18, which compares the total electrical power supplied by the traction substations with and without RES. As shown in Figure 18, the peak total power supplied by the TPSSs decreases from 13.22 MW without RES to 10.61 MW with RES operating near full capacity, that is, approximately 20% less power is drawn from the mains due to the contribution of the renewable generators. When comparing the individual TPSSs, as shown in Figure 19 and Figure 20, the percentage decrease in power demand over the travel time interval is even higher, drastically decreasing the duration of TPSS overloads (the power rating of TPSSs on high speed lines is typically 5.4 MW [1]). Considering the difference in total power demand and that the crossing between TPSSs occurs in 241 seconds, the overall energy

savings due to the renewable generators amount to approximately 200 kWh when both trains simultaneously travel at maximum speed.

6.2 One train traveling at maximum speed on the down-line

In this scenario the contribution of the renewable generators can be best appreciated. The voltage and traction power absorption profiles can be deduced from Figure 16 and Figure 17. For conciseness, the power supplied by the traction substations are compared in the following.

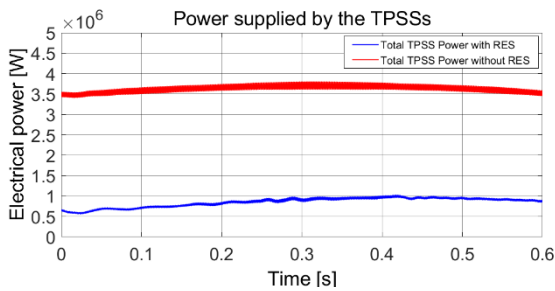


Figure 21: Total TPSS power with and without RES.

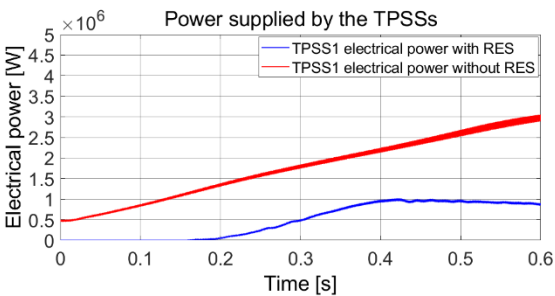


Figure 22: TPSS 1 power with and without RES.

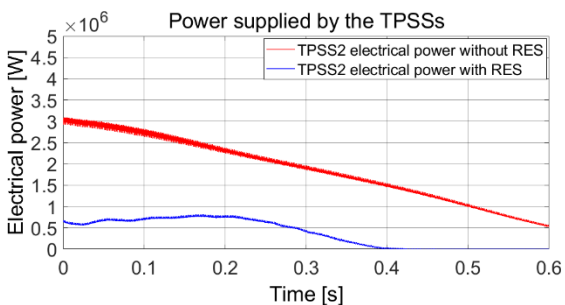


Figure 23: TPSS 2 power with and without RES.

As shown in Figure 22 and Figure 23, in this scenario each TPSS is not called into action for about one-third of the train crossing time, as the power demand of the traction load is met covered by the renewable generators. Moreover, according

to Figure 21, the maximum total power supplied by the TPSSs is 1 MW, compared to 3.72 MW without RES, which corresponds to a 73% decrease in peak power demand, highlighting the advantages in terms peak shaving capabilities given by the integration of RES into the power supply of the traction circuit.

Regarding the renewable generators, the following figures illustrate the electrical power generated by PV field and by the wind farm in response, respectively, to the chosen solar irradiance and wind speed profiles.

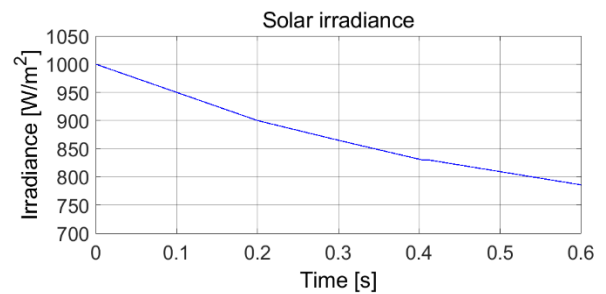


Figure 24: Solar irradiance

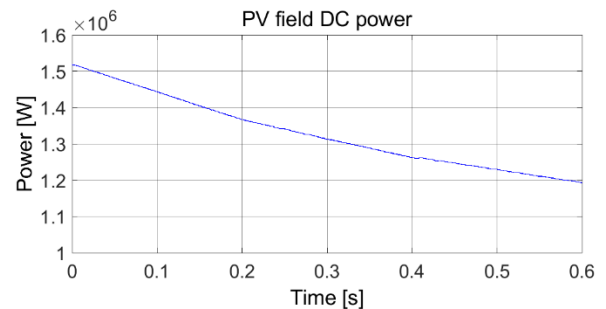


Figure 25: PV field electrical power generation

As evidenced by Figure 24 and Figure 25, the DC power produced by the PV field closely matches the solar irradiance profile by virtue of the MPPT algorithm implemented by means of the power converters described for this system.

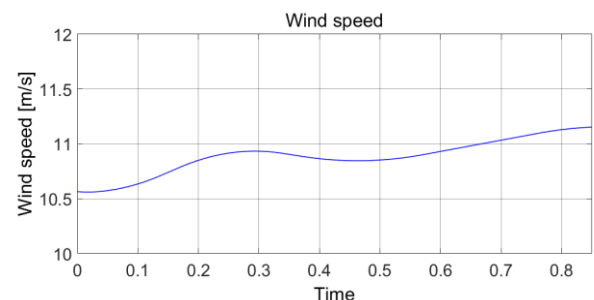


Figure 26: Wind speed profile

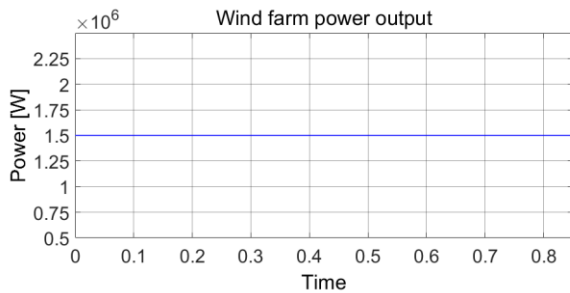


Figure 27: Wind farm electrical power output.

The simplified model adopted for the wind generators is seen to effectively limit the power output to the rated value (1.5 MW) whenever the wind speed is greater than the rated wind speed (10 m/s), as shown in Figure 26 and Figure 27.

7. Conclusions

The simulations conducted on the 3 kV railway system first without, and then with the connection of solar and wind generators at the traction substations have highlighted the contribution of the renewable generators to the power supply of the traction loads in different operating scenarios, and the convenience of their associated DC connection to the 3 kV DC railway system. With the integration of PV and wind generators operating around full capacity, the total power supplied by the TPSSs was seen to decrease from 3.72 MW to 1 MW, i.e., by 73%, in the case of one train traveling at maximum speed on the downhill track, and by 20% (from 13.22 MW to 10.61 MW) in the case of the railway section occupied by two trains traveling at maximum speed, leading to energy savings of approximately 200 kWh for each crossing between adjacent traction substations. Considering the railway traffic associated with high-speed lines and the high number of traction substations, the integration of renewable energy sources in conjunction with energy storage systems into the railway power supply could lead to significant energy savings and reduction in contracted power of railway systems. In addition, although the renewable generators partly cover the power demand of the traction loads, the continuity of service of the traction system albeit at a lower power level, would be favored in the event of TPSS fault or service interruption.

Several other analyses are necessary to evaluate the feasibility of the integration of renewable

generators into the 3 kV DC traction system, most notably regarding the implementation of energy storage and energy management systems that are of paramount importance to utilize the energy produced by wind and solar generators in the absence of power demand from the loads and to smoothen the power absorption from the grid-side. Other necessary studies include system reliability and fault analyses that are needed to evaluate short-circuit currents and the necessary protection switchgear, as well as economic feasibility analyses that are beyond the scope of this work.

8. Bibliography

- [1] M. Brenna, F. Foiadelli, and H. J. Kaleybar, "The Evolution of Railway Power Supply Systems towards Smart Microgrids", *IEEE Electrification Magazine*, 2020.
- [2] A. Biancucci, "Rotabili di trazione attuale e di moderna concezione", [PowerPoint slides], Trenitalia – direzione tecnica, <http://www.cifi.it/UpIDocumenti/Firenze16112018/Intervento%20Ing.%20Biancucci.pdf>, 2018.
- [3] R. F. Boehm, H. Yang, and J. Yan, *Handbook of Clean Energy Systems, Volume 1, Renewable Energy*, West Sussex: John Wiley & Sons Ltd, 2015.
- [4] W. Cao, Y. Xie, and Z. Tan, "Wind Turbine Generator Technologies", in *Advances in Wind Power*. London, United Kingdom: IntechOpen, 2012.